Membrane Tension Directly Shifts Voltage Dependence of Outer Hair Cell Motility and Associated Gating Charge

Seiji Kakehata and Joseph Santos-Sacchi

Sections of Otolaryngology and Neurobiology, Yale University School of Medicine, New Haven, Connecticut 06510 USA

ABSTRACT   The unique electromotility of the outer hair cell (OHC) is believed to promote sharpening of the passive mechanical vibration of the mammalian basilar membrane. The cell also presents a voltage-dependent capacitance, or equivalently, a nonlinear gating current, which correlates well with its mechanical activity, suggesting that membrane-bound voltage sensor-motor elements control OHC length. We report that the voltage dependence of the gating charge and motility are directly related to membrane stress induced by intracellular pressure. A tracking procedure was devised to continuously monitor the voltage at peak capacitance (V_{pkCm}) after obtaining whole cell voltage clamp configuration. In addition, nonlinear capacitance was more fully evaluated with a stair step voltage protocol. Upon whole cell configuration, V_{pkCm} was typically near −20 mV. Negative patch pipette pressure caused a negative shift in V_{pkCm}, which obtained a limiting value near the normal resting potential of the OHC (~−70 mV) at the point of cell collapse. Positive pressure in the pipette caused a positive shift that could reach values greater than 0 mV. Measures of the mechanical activity of the OHC mirrored those of charge movement. Similar membrane-tension dependent peak shifts were observed after the cortical cytoskeletal network was disrupted by intracellular dialysis of trypsin from the patch pipette. We conclude that unlike stretch receptors, which may sense tension through elastic cytoskeletal elements, the OHC motor senses tension directly. Furthermore, since the voltage dependence of the OHC nonlinear capacitance and motility is directly regulated by intracellular turgor pressure, we speculate that modification of intracellular pressure in vivo provides a mechanism for controlling the gain of the mammalian "cochlear amplifier".

INTRODUCTION

The term "cochlear amplifier" has been used to describe a physiologically vulnerable process that enhances near-threshold auditory sensitivity (Davis, 1983). In recent years, the outer hair cell (OHC) from the organ of Corti has been acknowledged to play a pivotal role in this process (see Dallos, 1992). The OHC is capable of voltage-dependent mechanical responses that appear to provide feedback into the basilar membrane, thereby sharpening the passive mechanical vibration of the cochlear partition (Brownell et al., 1985; Ashmore, 1987; Santos-Sacchi and Dilger, 1988; Ruggero, 1992). The cell also possesses a nonlinear gating charge movement or equivalently, a voltage-dependent capacitance, which correlates well with its mechanical activity (Ashmore, 1990; Santos-Sacchi, 1990, 1991). The similarity between characteristics of OHC nonlinear capacitance and OHC movement indicates that membrane-bound voltage sensor-motor elements control OHC length (Santos-Sacchi, 1990, 1991, 1993; Ashmore, 1992; Dallos et al., 1991; Iwasa, 1994). Indeed, estimates of the membrane-bound charge density of the OHC responsible for the nonlinear capacitance (7500 e⁻/mm²; Huang and Santos-Sacchi, 1993) coincide fairly well with estimates of the density of OHC intramem-

branous particles, the putative sensor-motor elements, observed electronmicroscopically (6000/mm²; Forge, 1991).

We have been studying the voltage dependence of the nonlinear capacitance of the OHC and have found that the voltage at peak capacitance (V_{pkCm}), which corresponds to the voltage of maximal motile sensitivity or gain, varies among cells and within single cells during recording under whole cell voltage clamp (Santos-Sacchi et al., 1994). This voltage can range from 0 mV to potentials near the normal resting potential of the OHC in vivo, namely about −70 mV (Dallos et al., 1982). We report here that this variability of the nonlinear capacitance as well as the voltage dependence of OHC movement is directly related to intracellular turgor pressure. Notably, a reduction of turgor pressure induces graded increases in nonlinear capacitance and negative voltage shifts in sensor/motor function. Furthermore, the effects of turgor pressure are not directly mediated through cytoskeletal linkages with the membrane voltage sensor, since digestion of the cortical cytoskeleton with intracellular trypsin does not abolish the effects of turgor pressure-induced membrane tension. A preliminary account of this work has been presented (Santos-Sacchi and Kakehata, 1994).

MATERIALS AND METHODS

OHCs were freshly isolated from the organ of Corti of the guinea pig cochlea (Kakehata et al., 1993), and were whole cell voltage clamped using an Axon 200B amplifier with patch pipettes having initial resistances of 2–3 MΩ, corresponding to tip sizes of 1–2 μm (Hamill et al., 1981). Residual series resistance (after electronic compensation) ranged from 3 to 7 MΩ. The removal of nonlinear ionic conductances is crucial in evaluating nonlinear capacitive currents. In the presence of nonlinear ionic conductances, voltage-induced currents may possess ionic as well as capacitive components, thereby making extraction of gating charge difficult or impossible.

Therefore, ionic blocking solutions were used to remove voltage-dependent ionic conductances so that capacitive currents could be analyzed in isolation (Santos-Sacchi, 1991; Huang and Santos-Sacchi, 1993). The patch pipette solution contained (in mM): 140 CsCl, 2 MgCl$_2$, 10 EGTA, and 10 HEPES, with pH 7.2 and osmolarity (adjusted with dextrose) noted in figure legends. The external solution contained (in mM): 100 NaCl, 20 TEA, 20 CsCl, 2 CoCl$_2$, 1.52 MgCl$_2$, 10 HEPES, and 5 dextrose, pH 7.2, 300 mOsm. Drugs were applied using the "Y-tube" method (Murase et al., 1990), during simultaneous whole chamber perfusion. Experiments were performed at room ter..perature.

A tracking procedure was developed to continuously monitor V_{pkCm} after obtaining whole cell configuration. The procedure utilizes a voltage stimulus protocol where equal but opposite polarity voltage pulses are delivered to the cell and the generated currents summed to extract nonlinear gating currents, as originally developed to measure ionic channel gating charge ($\pm P$ protocol, ± 40 mV; Armstrong and Bezanilla, 1973; Keynes and Rojas, 1974). Averages of three to five paired pulses were used. While the term "gating current" is typically applied to nonlinear currents associated with voltage sensor activity during ionic channel gating, we use this term for the motility-related voltage sensor displacement currents to indicate a similar molecular transduction strategy (see Alkon et al., 1993). Fig. 1A is an electrical model simulation of OHC voltage-dependent capacitance showing gating current traces obtained with this protocol. When the holding potential is more hyperpolarized than V_{pkCm}, the gating current consists of an initial upward (outward) transient current followed by a downward (inward) transient at voltage step offset. The polarity of the current reverses when the holding potential is more depolarized than V_{pkCm}. To track V_{pkCm}, holding potential (V_{hold}) was automatically decreased in 2 mV steps until a reversal of gating current polarity was obtained, thereupon V_{hold} was increased in 2 mV steps until polarity reversed again. Thus, V_{hold} was varied to follow gating current reversals, namely, V_{pkCm}. Tracking was always initiated from a holding potential of 0 mV. Since initial voltage conditions do not appear

to alter the voltage dependence of the OHC gating currents and the charge moved demonstrates no immobilization (see Fig. 5; Santos-Sacchi, 1991), the tracking technique should not interfere with V_{pkCm} measures. Fig. 1B presents data from an OHC illustrating the procedure. The program Clampex (Axon Instruments, CA) was modified to perform the V_{pkCm} tracking procedure online, and holding potential was corrected for the effects of residual series resistance. Peak capacitance ($C_{m\ Pk}$) values were also monitored during the tracking procedure using transient analysis of capacitive currents induced by a -10 mV step. Detailed evaluation of total membrane capacitance was made at different potentials by transient analysis of currents induced by a voltage stair step stimulus, and the capacitance function was fit to the first derivative of a two state Boltzmann function relating nonlinear charge to membrane voltage ($\delta Q/\delta V$; Santos-Sacchi, 1991; Huang and Santos-Sacchi, 1993),

$$C_m = Q_{max}\frac{ze}{kT}\frac{b}{(1+b)^2} + C_{lin} \tag{1}$$

where

$$b = \exp\left(\frac{-ze\,(V-V_{pkCm})}{kT}\right) \tag{2}$$

Q_{max} is the maximum nonlinear charge moved, V_{pkCm} is voltage at peak capacitance or equivalently, at half-maximal nonlinear charge transfer, V_m is membrane potential, z is valence, C_{lin} is linear membrane capacitance, e is electron charge, k is Boltzmann's constant, and T is absolute temperature. Series resistance, R_s was estimated from the decaying time constant and integrated charge of the voltage step-induced current, as fully described elsewhere (Santos-Sacchi, 1993; Huang and Santos-Sacchi, 1993). This technique is relatively insensitive to the effects of data filtering. Membrane resistance, R_m, was evaluated from steady state current. C_{lin} was estimated from the fit to above capacitance (C_m) equation, and indicates the intrinsic linear capacitance of the membrane upon which rides the bell-shaped voltage-dependent capacitance (C_v). All analysis techniques have been previously detailed in Huang and Santos-Sacchi (1993). Pipette pressure was modified with a syringe connected to the Teflon tubing attached to the patch pipette holder. Pressure was monitored via a T-connector to a pressure monitor (WPI, Sarasota, FL). Modifications of intracellular pressure have been shown to modulate OHC membrane tension (Iwasa and Chadwick, 1992; Iwasa, 1993), and as an indicator of pressure-induced membrane stress we present longitudinal strain measures (which are linearly related to membrane stress for small deformations (Iwasa and Chadwick, 1992). All experiments were videotaped using a Matrox (Montreal, Quebec, Canada) video overlay board which combines an enhanced graphics adaptor and video. Measures of voltage-induced (20 mV increments) mechanical responses were made off the video monitor with a differential optoresister technique (Santos-Sacchi, 1989, 1991). Mechanical data were fit to a two state Boltzmann function to determine the voltage at maximum sensitivity ($V_{\delta L\ max}$). All data analysis was performed with the software package MATLAB (Mathworks, Natick, MA).

RESULTS

The isolated in vitro OHC possesses a positive intracellular turgor pressure of about 1 kPa (Ratnanather et al., 1993; Chertoff and Brownell, 1994). Thus, when a normally cylindrical OHC is under tight-seal whole cell recording, especially with large tipped pipettes, there exists a potential path through the pipette for the release of intracellular pressure, and the cell may depressurize. Fig. 2 illustrates the effect of reducing intracellular pressure during the course of whole cell recording on V_{pkCm} where depressurization of the OHC is assisted by an osmotic imbalance between pipette solution and extracellular media (Δ mOsm = -14). To indicate the effectiveness of pressure changes, longitudinal strain was calculated ($\delta z = (l - L)/L$, where L is initial
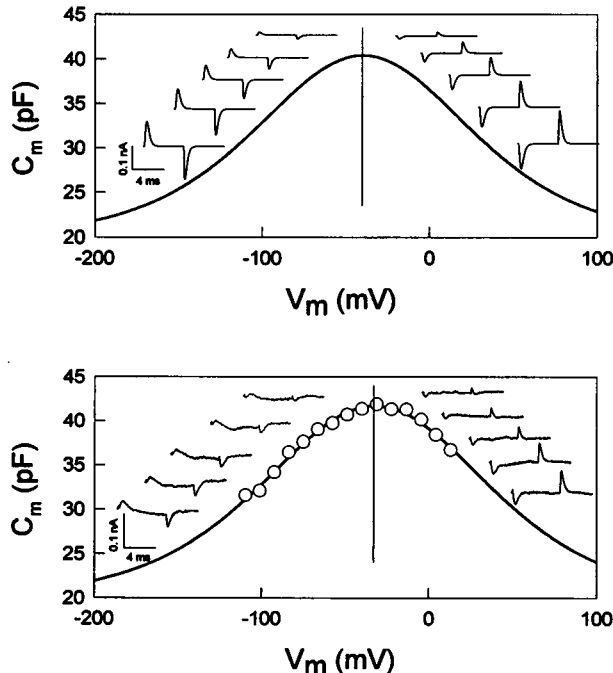

FIGURE 1   Illustration of underlying principle of V_{pkCm} tracking technique. (A) An electrical model simulation of OHC capacitance (that of Huang and Santos-Sacchi, 1993) showing traces obtained with the $\pm P$ protocol (2 mV holding potential alterations about V_{pkCm}). (B) Capacitance of an OHC (measured with the voltage stair step protocol; Huang and Santos-Sacchi, 1993) illustrating the same technique. Note the reversal of gating currents as the holding voltage passes through the region of peak capacitance. Osmolarity of the intracellular solution was 300 mOsm.
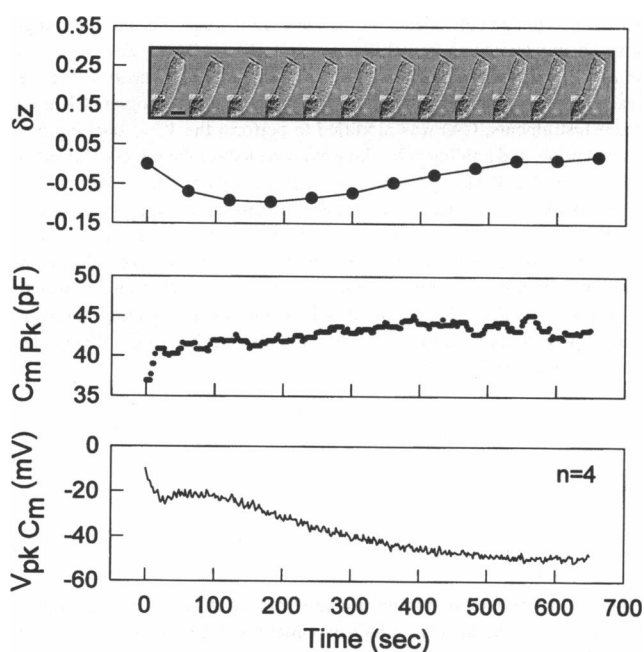
FIGURE 2   Effect of cell turgor reduction on OHC longitudinal strain, δz (*top*), peak capacitance (*middle*) and V_{pkCm} (*bottom*), utilizing the tracking technique, as a function of time after obtaining whole cell voltage clamp configuration (average of four cells; R_s:7.2 MΩ; R_m:177 MΩ). Initial cell length was 55.5 ± 4.1 μm (mean ± SE). (*Inset, top*) Video images at 1-min intervals illustrate the shape changes of one of the OHCs. Scale bar 10 μm. Osmolarity of the intracellular and extracellular solutions in these cells was 286 and 300 mOsm, respectively. Whole cell configuration was obtained by electrical "zapping" (see Discussion). Cells did not collapse during the recording period.

length, and l is the length of the cell when deformed), and presented as well. The length of the OHC correlates well with turgor pressure (positive pressure reduces length and increases the radius; Chertoff and Brownell, 1994; Iwasa, 1993). The averaged time course of V_{pkCm} in four cells from the third cochlear turn indicates a shift from an initial value of −21.5 mV to a steady state value of −49.3 mV at 10 min. In addition, $C_{m\ Pk}$ increased from an initial value of 40.9 to 43.1 pF. Cell length was reduced immediately after entering the cells, but slowly recovered to initial levels, indicating that over the course of the 10 min recording turgor pressure decreased. During this time the cell did not collapse, and mechanical responses remained robust (however, see below). In four other cells, a more complete analysis of cell capacitance was performed using a voltage stair step protocol (see Materials and Methods). A fit to these capacitance data provided initial/steady state fitted parameters of (mean ± SE), as follows. Q_{max}: 2.41 ± 0.18/3.73 ± 0.3; V_{pkCm}: −17.0 ± 6/−54.5 ± 3.5; z: 0.73 ± 0.04/0.71 ± 0.02; C_{lin}: 21.4 ± 1.5/19.5 ± 2.3. Average electrode series resistance and membrane resistance were 4.0 and 315 MΩ, respectively. The slow negative shift in voltage dependence is not due to the dissipation of a diffusion potential at the pipette tip, for the following three reasons. 1) Whereas the time course for osmotic stress effects were on the order of 10 min, diffusion potentials are typically dissipated within 3 min, as the pipette

solution and cell solution equilibrate. Indeed, under current clamp with KCl solutions (140 mM), OHCs that initially have resting potentials greater than −20 mV attain potentials near −70 mV within 20–30 s after whole cell configuration. This is believed to reflect a restoration of intracellular potassium after depletion accompanying OHC isolation (Ashmore and Meech, 1986; Santos-Sacchi and Dilger, 1988). The immediate reduction of cell length noted upon entering whole cell configuration is probably due to clamping the cell at 0 mV at the onset of tracking, and the subsequent rapid exchange of pipette and cell solutions. 2) With small tipped pipettes (10 MΩ; 0.5 μm tip) containing isoosmolar solutions, although the initial decrease in cell length occurred, no subsequent negative shifts of V_{pkCm} were observed over periods of 30 min or longer. 3) As shown below, pipette pressure changes were as effective as osmotic treatments. Thus, we find an increase in maximum nonlinear charge moved, and a slight decrease in linear capacitance as intracellular pressure and, correspondingly, membrane tension is dissipated. The decrease in linear capacitance might be expected because of a reduced stretch on the plasma membrane.

To investigate the effects of turgor pressure more directly, the intracellular pressure of OHCs was directly modified through the patch pipette. Fig. 3 illustrates the reversible effects of decreasing intracellular pressure on V_{pkCm} and cell capacitance. V_{pkCm} became more negative and the magnitude of peak capacitance grew as the pressure was decreased; subsequently, an increase of pressure reversed the effects. Stable values of V_{pkCm} could be attained with constant pipette pressure, although we do not claim that pipette pressure actually clamps the intracellular pressure. Indeed, during stable pipette pressure, modification of extracellular osmolarity produced results similar to those obtained with pipette pressure changes; namely, hyperosmotic media caused negative
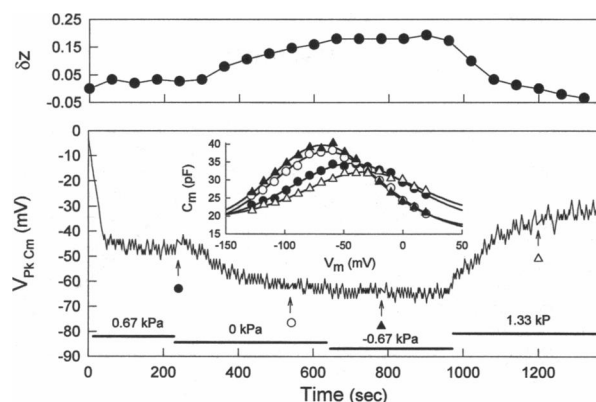

FIGURE 3   OHC longitudinal strain, δz (*top*), V_{pkCm} (*bottom*), and nonlinear capacitance (*inset*) at different pipette pressures. Initial cell length was 38.5 mm. This cell collapsed at −0.67 kPa, and longitudinal mechanical responses stopped. Responses returned upon delivery of positive pressure. R_s: 4.1 MΩ, R_m: 221 MΩ. Fits (*insets, solid lines*) for capacitance indicate V_{pkCm}, Q_{max}, z, and C_{lin} of −43.6 mV, 2.56 pC, 0.71, and 17.0 pF (@ 0.67 kPa); −64.28 mV, 3.18 pC, 0.76, and 14.2 pF (@ 0 kPa); −68.14 mV, 3.02 pC, 0.82, and 15.6 pF (@ −0.67 kPa); −32.4 mV, 1.95 pC, 0.72, and 18.57 pF (@ 1.33 kPa). Osmolarity of the intracellular solution was 286 mOsm.

voltage shifts, and hypoosmotic media caused positive voltage shifts (data not shown). OHC δz changes mirrored those of V_{pkCm}. Fig. 4 illustrates, in another cell, that below a critical negative pipette pressure where the OHC just collapses, V_{pkCm} remains constant. This potential is likely to reflect the true voltage dependence of the motility voltage sensor/effector because there is no tension on the membrane motor at the point of cell collapse. In nine cells, this potential was -65.5 ± 1.2 mV (mean $\pm$ SE), which is close to that of the resting potential of OHCs in vivo (Dallos et al., 1982). In some cases where the OHC not only lost its cylindrical shape, but flattened, the magnitude of peak capacitance decreased somewhat ($\sim 10\%$). This may have been due to resultant space clamp problems.

The cylindrical OHC has an elaborate cytoskeletal network linked to the plasma membrane (Holley and Ashmore, 1990; Forge, 1991), and it is conceivable that intracellular pressure works via this network to induce tension on the motility voltage sensors. To evaluate this possibility, we included trypsin (300 μg/ml) in the pipette solution (300 mOsm). This treatment is known to digest and/or disrupt the OHC cortical cytoskeleton, and produce a spherical cell whose plasma membrane is essentially free of cytoskeletal attachments, while leaving the voltage sensor fully functional (Huang and Santos-Sacchi, 1994). Fig. 5 illustrates the effect of intracellular pressure on V_{pkCm} and peak membrane capacitance of an OHC during the course of trypsin treatment. In more than 10 cells studied, V_{pkCm} initially shifted to negative potentials after whole cell configuration, but after about 10 min it shifted slowly to positive potentials. This positive shift coincided with the onset of trypsin-induced structural changes and is likely to reflect a growing tension on the membrane as the cell swelled into a sphere. Normally, C_{mPk} remains stable during trypsin treatment (Huang and Santos-Sacchi, 1994). However, in this case, at 14.5 min the electrode and cell were moved to position the cell so that pressure could be delivered without losing the seal. An immediate decrease in peak capacitance was noted, probably because of an induced membrane tension during the manipulation (Fig. 5, *bottom*). In this particular case, the cell became fully spherical at about 15 min, whereupon positive pipette pressure steps further shifted V_{pkCm} in the positive

direction and reduced peak capacitance, in a reversible manner. Subsequently, negative pressure restored peak capacitance to original levels, and only after the pipette was visibly clear of cellular debris could positive pipette pressure again shift V_{pkCm} to positive values. (In this case, and three others, although $C_{m\,Pk}$ increased with negative pipette pressure, V_{pkCm} did not change. We believe that this occurred because the magnitude of nonlinear charge movement is more susceptible to pressure effects than V_{pkCm}. In Fig. 5, the pipette became plugged with cellular debris upon delivery of negative pressure, and it is likely that the full negative pipette pressure was not delivered to the cell. Upon subsequent delivery of positive pipette pressure, which unplugged the tip, it can be seen that $C_{m\,Pk}$ decreased before a positive shift in V_{pkCm} ensued. Alternatively, it may be possible that the limiting voltage shift of V_{pkCm} became more positive with trypsin treatment. We are currently investigating this possibility.) Finally, the cell burst at a pipette pressure of about 1 kPa and V_{pkCm} of $+8$ mV. From these types of observations, in 10 cells out of 12, we conclude that membrane tension directly modulates the embedded motility voltage sensor.

A correspondence between OHC nonlinear capacitance and motility voltage dependence has been observed (Santos-Sacchi, 1991). Voltage at half maximal charge movement, V_h (or equivalently, V_{pkCm}), corresponds to the voltage where OHC mechanical responses are maximally voltage sensitive, $V_{\delta L\;max}$. We further demonstrate a close relationship between OHC membrane capacitance and movement under different pressure conditions within individual cells. The inset in the bottom panel of Fig. 6 depicts the structure of an OHC under two different pipette pressure conditions, $+0.54$ and -0.19 kPa. Positive pressure caused the cell to shorten, whereas negative pressure caused the cell to lengthen. Fig. 6 shows that the voltage dependence of OHC motility essentially mirrors that of the nonlinear capacitance of the cell. Both shifted to hyperpolarized levels as intracellular pressure was decreased. In three cells, $V_{\delta L\;max}$ was (mean $\pm$ SE) -23.6 ± 2.9 mV and V_{pkCm} was -24.7 ± 4.2 mV for a high pipette pressure condition $(0.49 \pm 0.1$ kPa); a reduced pipette pressure $(-0.05 \pm 0.07$ kPa) shifted these values to -45.7 ± 2.2 mV and -56.5 ± 4.8 mV, respectively. Slight differences may be due to changes in intracellular pressure during the interval

FIGURE 4 Pipette pressure versus V_{pkCm} (*bottom left*), OHC longitudinal strain, δz (*middle left*), and peak capacitance (*top left*). R_s: 7.5 MΩ, R_m: 150 MΩ. Initial cell length was 69.7 μm. In this case, the cell collapsed at -1.33 kPa. *Right* plot of means of V_{pkCm} (●) and peak capacitance (○) obtained during the last 12 s of pressure durations. Osmolarity of the intracellular and extracellular solutions was 300 mOsm.
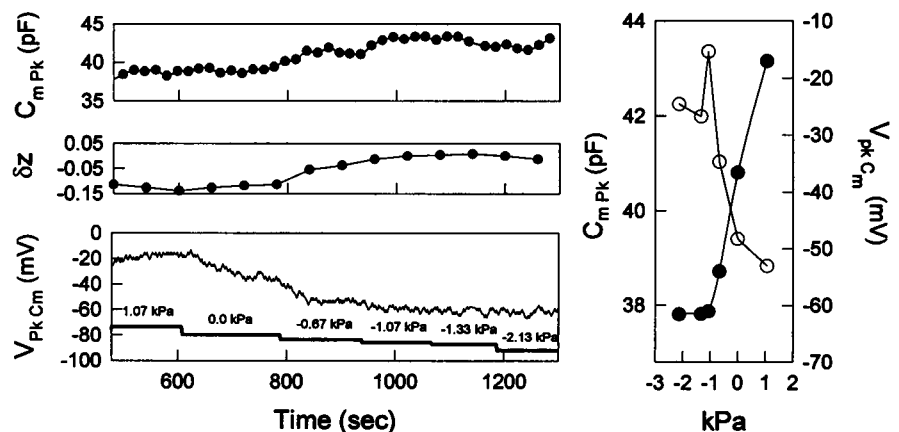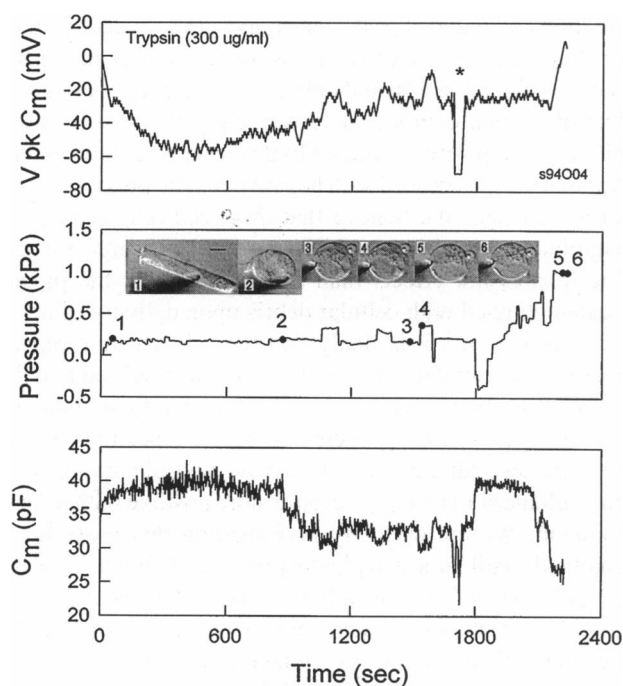
FIGURE 5   Effects of intracellular trypsin treatment on V_{pkCm} (*top*) and $C_{m\,pk}$ (*bottom*). (*middle*) Pipette pressure delivered, sampled every 8 s. The numbered inset images are from selected time periods corresponding to the numbered solid circles on the pressure trace. Scale bar is 10 μm. During constant pipette pressure, V_{pkCm} initially declines but shifts to hyperpolarized levels when cell structural changes ensue, around 10 min. After the OHC reached a spherical shape, positive pipette pressure induced positive voltage shifts and decreases in peak capacitance. At the point indicated by the asterisk, the holding potential was maintained at about $\sim$70 mV to evaluate the effect of initial conditions on V_{pkCm}. After the release of holding potential, V_{pkCm} quickly shifted back to its previous value, indicating that holding potential does not influence V_{pkCm}. At 30 min, negative pressure is delivered and $C_{m\,Pk}$ increased to initial levels, but the electrode subsequently became plugged. Only after considerable attempts to unplug the pipette with positive pressure were we able to observe the release of cellular debris from the tip. At that point V_{pkCm} began to shift to depolarized levels and $C_{m\,Pk}$ decreased; the cell finally burst after reaching a steady state V_{pkCm} of +8 mV for about 20 s.

($\sim$1–2 min) between nonlinear capacitance measurement (stair step protocol) and mechanical response measures (voltage pulse protocol). The correspondence between voltage dependencies indicates that motor and sensor are either tightly coupled or one entity. The singular identity of motor and sensor is further indicated by the co-localization of the two within a restricted region of the lateral plasma membrane (Dallos et al., 1991; Huang and Santos-Sacchi, 1993, 1994).

Fig. 6 also illustrates that negative pipette pressure reduces the maximum mechanical response of the OHC (Santos-Sacchi, 1991). Despite this reduction, however, the inset in the top panel of Fig. 6 illustrates that the maximum mechanical gain of the cell can remain essentially unaltered. That is, in this example, the maximum gain remained near 20 nm/mV under both pressure conditions.

Interestingly, lanthanides, which interfere with OHC osmotic pressure regulation (Crist et al., 1993; however, see Chertoff and Brownell, 1994), possibly via interaction with

OHC stretch receptors (Yang and Sachs, 1989; Iwasa et al., 1991; Ding et al., 1991) also shifted V_{pkCm} (Fig. 7). Lanthanides have been shown to reversibly block OHC motility and nonlinear gating charge (Santos-Sacchi, 1991). Extracellularly applied lutetium chloride (100 μM), one of the lanthanides tested, shifted V_{pkCm} to hyperpolarized levels and decreased peak capacitance only slightly. At a higher concentration (1 mM), however, it apparently shifted V_{pkCm} in the opposite direction but reduced the nonlinear capacitance markedly (Fig. 7, *inset*). Mechanical responses were fully blocked, as well, without cell collapse. Such a large drop in nonlinear capacitance may invalidate the tracking technique so that the shift to positive potentials is likely artifactual. In all cases of lanthanide treatment where nonlinear capacitance block was not complete, i.e., where V_{pkCm} could be evaluated unequivocally, tracking and full analysis with the voltage stair protocol indicated a V_{pkCm} shift to negative potentials, opposite that of potential charge screening effects. Lanthanides also increased cell length, similar to treatments that reduced turgor pressure. In three cells, 1 mM lutetium increased OHC length about 5%. It was of interest to determine whether lanthanides could interfere with the effects of membrane tension on nonlinear capacitance. Fig. 8 illustrates that turgor pressure changes remained capable of reversibly shifting V_{pkCm} and altering Q_{max} in cells that were treated with both
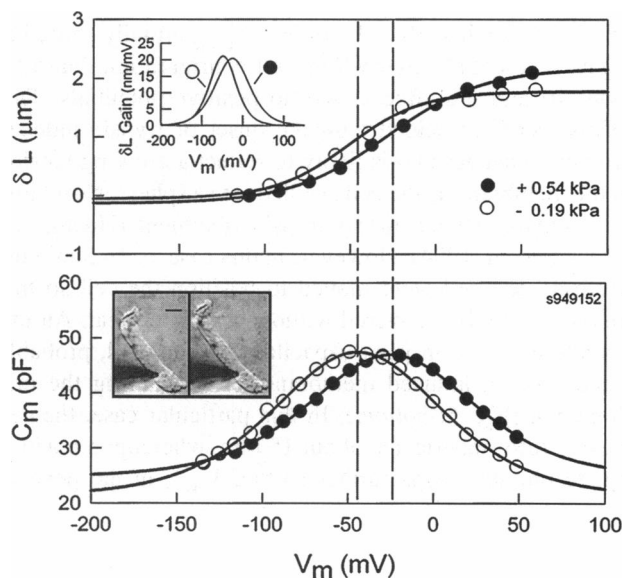

FIGURE 6   Membrane capacitance (*bottom*) and movement (*top*) of an OHC under different pressure conditions delivered through the pipette. Length changes induced by 20 mV steps from −140 to +60 mV (nominal), but corrected for series resistance effects in figure. R_s: 3.5 MΩ, R_m: 154 MΩ @ 0.54 kPa, and R_s: 2.0 MΩ, R_m: 88 MΩ @ −0.19 kPa. Fits (positive vs. negative pressure) for capacitance indicate V_{pkCm}, Q_{max}, z, and C_{lin} of −24.7 mV, 2.87 pC, 0.79, and 24.8 pF versus −44.2 mV, 3.47 pC, 0.77, and 21.3 pF. Fits (positive vs. negative pressure) for mechanical data indicate V_h (voltage midpoint) and z of −28.0 mV and 0.91 versus −51.1 mV and 1.2. Dotted lines indicate V_{pkCm} under each condition. (*Inset, top*) First derivative of the fitted mechanical responses, indicating the gain of the mechanical response under the two pressure conditions. (*Inset, bottom*) Video images of OHC at high (*left*) and low (*right*) pressures. Scale bar: 10 μm. Osmolarity of the intracellular and extracellular solutions was 300 mOsm.

trypsin and lutetium. This indicates that the activity of stretch receptors, which are blocked by low micromolar concentrations of lanthanides, is not responsible for stress-induced effects on OHC membrane capacitance.

DISCUSSION

Treatments that reduce OHC turgor are known to decrease the magnitude of electromotility (Brownell et al., 1989; Shehata et al., 1991). Indeed, we have previously shown that collapsing the OHC with negative pipette pressure produces a rapid and reversible loss of longitudinal motility, but the function of the motility voltage sensor remains intact (Santos-Sacchi, 1991). In fact, we reported that the magnitude of the nonlinear charge movement increased by about 10% under the negative pressure condition, corresponding to the increase in C_{mPk} that we now observe upon reduced cell turgor. Iwasa (1993) first systematically studied the effects of membrane tension on OHC capacitance, and found that increased turgor pressure decreased nonlinear capacitance measured at three fixed holding potentials. He correctly concluded, based on modeling the data, that membrane tension caused a positive shift in V_{pkCm}. More recently, Gale and Ashmore (1994a) showed that V_{pkCm} shifted to a depolarized level and peak capacitance decreased when positive pressure was applied via the patch pipette. However, they further reported that upon collapse of the cell with hyperosmotic extracellular media, V_{pkCm} remained unchanged (-36 ± 11 mV; mean $\pm$ SD), but voltage-dependent capacitance decreased some 60–70%. Other differences are apparent between their results and ours. First, no change in linear capacitance was observed by them during pressure increases, and second, while we find either little change or a slight decrease in z during positive pressure conditions, perusal of their data indicates a marked increase. Notably, Gale and Ashmore (1994a) did not employ ionic channel blockers, and used a phase tracking technique that can be susceptible to changes in electrode and/or membrane resistance. Changes in OHC membrane resistance can be quite large under those conditions, where outward potassium currents can reach several nA.
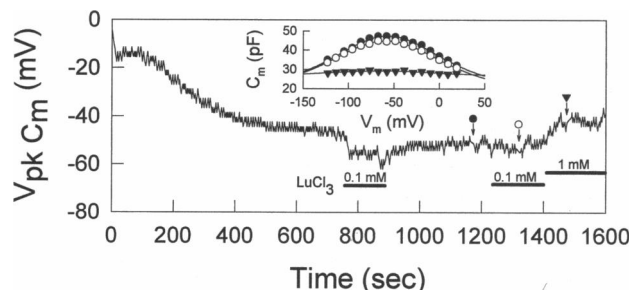
FIGURE 7   Effects of lanthanides on V_{pkCm} and nonlinear capacitance. After V_{pkCm} stabilized, lutetium chloride (1 mM) was applied extracellularly using a Y-tube delivery system. Inset shows voltage-dependent capacitance obtained by the voltage stair step technique (Huang and Santos-Sacchi, 1993). R_s: 6.5 MΩ, R_m: 145 MΩ. Fits (————) to the capacitance data indicate V_{pkCm}, Q_{max}, z, and C_{lin} of -56.9 mV, 4.1 pC, 0.67, and 20.9 pF ($\bullet$) and -58.9 mV, 4.1 pC, 0.63, and 19.4 pF (O). Data obtained with 1 mM lutetium chloride ($\blacktriangledown$) could not be fit reliably.
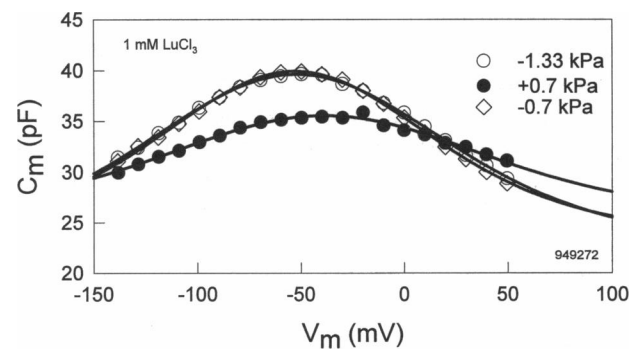
FIGURE 8   Effects of turgor pressure on nonlinear capacitance in a cell treated with intracellular trypsin and extracellular lutetium chloride (1 mM). Initial $C_{m\ Pk}$ was 47.5 pF, and in this cell only a partial block of nonlinear capacitance by lutetium was observed, enabling us to evaluate changes in V_{pkCm}. R_s: 2.5 MΩ, R_m: 300 MΩ. Reversible changes in cell capacitance induced by pressure modification are still observed. Fits (————) to the capacitance data indicate V_{pkCm}, Q_{max}, z, and C_{lin} of -52.0 mV, 3.4 pC, 0.52, and 22.5 pF (O): -1.33 kPa), and -38.6 mV, 2.2 pC, 0.47, and 25.3 pF ($\bullet$: $+0.7$ kPa), and -52.8 mV, 2.9 pC, 0.57, and 23.6 pF ($\Diamond$: -0.7 kPa).

Our work indicates that the variability of V_{pkCm} we initially noted (Santos-Sacchi et al., 1994) results from variability in OHC turgor pressure. Upon establishing whole cell configuration, OHC V_{pkCm} and $V_{\delta L\ max}$ are at a potential near -20 mV. Actually, this initial voltage depends on the method of obtaining whole cell configuration. Applying negative pressure to break the membrane patch can cause an immediate loss of cell turgor, whereas electrically breaking through the membrane patch (zapping) can prevent such a loss. The former technique produces a more negative initial V_{pkCm}. Subsequent to whole cell configuration, V_{pkCm} directly follows modifications of intracellular pressure, but shifts to a limiting negative voltage when depressurized. Before cell collapse, V_{pkCm}, and correspondingly, $V_{\delta L\ max}$ can attain potentials close to that of the resting potential of OHCs in vivo (Dallos et al., 1982). At this point, mechanical responses are still robust and maximum voltage-dependent movement will exist near normal resting potentials. It should be emphasized that despite the fact that reduced turgor pressure decreases the overall magnitude of the mechanical response (Fig. 6; and see Santos-Sacchi, 1991, Fig. 11), maximum gain or sensitivity is little affected before cell collapse (Fig. 4, inset). Thus, for an OHC at a normal resting potential, reducing turgor pressure effectively increases the mechanical gain at that potential. In fact, another mechanism may aid in aligning the resting potential and $V_{\delta L\ max}$ under normal conditions. It is known that increased turgor can hyperpolarize, and reduced turgor can depolarize the OHC via the action of potassium selective stretch receptors (Iwasa et al., 1991; Harada et al., 1993). Correspondingly, sustained hyperpolarization can increase turgor and depolarization can reduce turgor pressure (Shehata et al., 1991). Thus, lowering turgor pressure may cause $V_{\delta L\ max}$ and membrane potential to approach each other, thereby maximizing the mechanical responsiveness of the OHC to receptor potentials, which presumably drive OHC motility in vivo (Evans and Dallos, 1993).

One problem with the potential role of OHC motility as the basis for the cochlear "amplifier" is that the magnitude of the AC mechanical response induced by receptor potentials in the high frequency region near threshold is calculated to be 20 dB smaller than basilar membrane motion (Santos-Sacchi, 1989, 1992). This is based on prior in vitro observations that the mechanical sensitivity of the OHC is not maximal near the normal in vivo resting potential of -70 mV. This dilemma has prompted suggestions that other hair cell mechanisms, e.g., stereociliar mechanics, might provide sensory gain (Santos-Sacchi, 1989; Hudspeth and Gillespie, 1994). However, the magnitude of turgor pressure in vivo is unknown. If it were close to 0, this might alleviate the apparent disparity between the magnitudes of basilar membrane motion and OHC motion, since the mechanical gain of the OHC would be maximal near the normal resting potential of the cell. It is possible that the high intracellular turgor pressure that is found in isolated OHCs (Ratnanather et al., 1993) is a consequence of the isolation procedures, since it is often noted that OHCs swell because of increased cytoplasmic osmolarity when they are maintained in vitro (Chertoff and Brownell, 1994).

Recently, Kalinec et al. (1992) have shown, using light microscopic evaluation, that treatment of the OHC with intracellular trypsin caused the cell to round up, presumably because of digestion of the cytoskeleton of the cell. Interestingly, voltage-dependent mechanical responses were still present. We confirmed by using electronmicroscopy that the cytoskeleton was digested; we also determined that the voltage sensor remained fully functional (Huang and Santos-Sacchi, 1994). In the present study we used trypsin treatment to show that cytoskeletal elements are not responsible for the susceptibility of the voltage sensor to modification of intracellular pressure. Thus, unlike stretch receptors that may sense tension through an elastic cytoskeleton (Sokabe et al., 1991), the OHC voltage sensor appears to respond to tension delivered directly to the plasma membrane. The role of the cortical cytoskeleton in the OHC has been proposed to provide structural constraints that funnel integral membrane motor protein area changes into anisotropic mechanical responses of the whole cell, namely predominant length changes (Kalinec et al., 1992; Santos-Sacchi, 1993). However, we have preliminary evidence that the sensitivity of the membrane motor to changes in turgor pressure increases after destruction of the cortical cytoskeleton. That is, smaller changes in pipette pressure are required to influence nonlinear capacitance after the cytoskeleton is destroyed. Thus, in addition to providing constraints on motility, the cytoskeleton may normally buffer the effects of turgor pressure alterations.

The underlying mechanism responsible for the effects of membrane tension on the nonlinear capacitance of the OHC has been theoretically evaluated by Iwasa (1993, 1994). By supplementing a simple two state Boltzmann model with an elastic energy term, shifts in V_{pkCm} were evidenced upon changes in the elastic energy. However, whereas the voltage shifts are predicted, the changes observed experimentally in

the magnitude of the voltage-dependent capacitance when tension is modified (Fig. 3; Gale and Ashmore, 1994a) are not. The increase in the amount of charge moved as membrane tension is dissipated may represent an increase in the number (N) of voltage sensors/motors capable of conformational change within the membrane. We find that the distance traversed by the sensor in the membrane electric field remains constant, evidenced by a fairly stable z during pressure modifications. Thus, in addition to Iwasa's elastic energy term, perhaps the number of functional sensors is tension-dependent. This possible change in the number of functional sensor/motors might indicate, in turn, that the maximum OHC length change would increase as turgor pressure is dissipated. However, the opposite is the case (Fig. 6; Santos-Sacchi, 1991). One possible explanation for this discrepancy is that coupling of the voltage sensor to the effector is less efficient under reduced tension, resulting in a smaller membrane area change. Alternatively, the membrane area changes thought to be responsible for the overall mechanical response of the cell (Kalinec et al., 1992; Iwasa and Chadwick, 1992; Iwasa, 1993; Santos-Sacchi, 1993) may actually be enhanced, but the translation mechanism funneling area changes into length changes may be compromised. It may be possible to explore this issue by measuring voltage-dependent changes in membrane patch area under conditions of variable tension.

Lanthanides have some effects similar to turgor pressure reductions, including negative shifts of V_{pkCm} and increases in cell length. We initially suggested that lanthanides shifted V_{pkCm} to positive potentials because of charge screening effects on the extracellular aspect of the OHC membrane (Santos-Sacchi, 1991). However, it is now clear that those initial studies were influenced by turgor pressure effects, since in those studies the pipette series resistance was kept low by delivering transient positive and negative pressures. Thus, it is likely that the effects of pipette pressure alterations on OHC turgor masked the true effects of lanthanides. Gale and Ashmore (1994b) have recently presented data indicating that extracellular gadolinium shifts V_{pkCm} in the negative direction, in aggreement with our present results. They suggested that gadolinium charge screens from the inner aspect of the OHC membrane; however, it is unlikely that lanthanides enter the cell and charge screen on the intracellular aspect of the membrane, since intracellular EDTA-like calcium chelators, which both they and we used are far more effective (5–10 orders of magnitude) at buffering lanthanides (Kolthoff et al., 1969). While one mechanism of lanthanide action may involve interference with OHC osmo-regulation (Crist et al., 1993), clearly this cannot solely account for the reduction in nonlinear capacitance we observe, since induced turgor pressure changes continue to alter nonlinear capacitance in the presence of lanthanides. It is possible that lanthanides are capable of directly reducing tension on the membrane motors, perhaps via electrostatic effects. Further studies are required to resolve this issue.

In conclusion, our results indicate that OHC turgor pressure directly controls the voltage dependence of the nonlinear

capacitance and mechanical response of the cell, probably through direct induction of tension on the motility voltage sensor/effector. We speculate that modulation of turgor pressure in vivo, perhaps via OHC stretch receptor activity, may provide a unique mechanism for gain control of the cochlear "amplifier".

REFERENCES

Alkon, D. L., R. Etcheberrigaray, and E. Rojas. 1993. Distribution of voltage sensors in mammalian outer hair cells. *Biophys. J.* 65:1755–1756.

Armstrong, C. M., and F. Bezanilla. 1973. Currents related to movement of the gating particles of the sodium channels. *Nature.* 242:459–461.

Ashmore, J. F. 1987. A fast motile response in guinea-pig outer hair cells: the cellular basis of the cochlear amplifier. *J. Physiol.* 388:323–347.

Ashmore, J. F. 1990. Forward and reverse transduction in the mammalian cochlea. *Neurosci. Res. Suppl.* 12:S39–S50.

Ashmore, J. F. 1992. Mammalian hearing and the cellular mechanism of the cochlear amplifier. *In* Sensory Transduction. D. P. Corey and S. D. Roper, editors. Rockefeller University Press, New York, 395–412.

Ashmore, J. F., and R. W. Meech. 1986. Ionic basis of membrane potential in outer hair cells of guinea pig cochlea. *Nature.* 322:368–371.

Brownell, W. E., C. R. Bader, D. Bertrand, and Y. de Ribaupierre. 1985. Evoked mechanical responses of isolated cochlear outer hair cells. *Science.* 227:194–196.

Brownell, W. E., W. Shehata, and W. B. Imredy. 1989. Slow electrically and chemically evoked volume changes in guinea pig outer hair cells. *In* Biomechanics of Active Movement and Deformation of Cells. N. Akas, editor. Springer-Verlag, New York, 493–498.

Chertoff, M. E., and W. E. Brownell. 1994. Characterization of cochlear outer hair cell turgor. *Am. J. Physiol.* 266:C467–C479.

Crist, J. R., M. Fallon, and M. R. Bobbin. 1993. Volume regulation in cochlear outer hair cells. *Hearing Res.* 69:194–198.

Dallos, P. 1992. The active cochlea. *J. Neurosci.* 12:4575–4585.

Dallos, P., B. N. Evans, and R. Hallworth. 1991. On the nature of the motor element in cochlear outer hair cells. *Nature.* 350:155–157.

Dallos, P., J. Santos-Sacchi, and A. Flock. 1982. Intracellular recordings from outer hair cells. *Science.* 218:582–584.

Davis, H. 1983. An active process in cochlear mechanics. *Hearing Res.* 9:79–90.

Ding, J. P., R. J. Salvi, and F. Sachs. 1991. Stretch-activated ion channels in guinea pig outer hair cells. *Hearing Res.* 56:19–28.

Evans, B. N., and P. Dallos. 1993. Stereocilia displacement induced somatic motility of cochlear outer hair cells. *Proc. Natl. Acad. Sci. USA.* 90:8347–8351.

Forge, A. 1991. Structural features of the lateral walls in mammalian cochlear outer hair cells. *Cell Tissue Res.* 265:473–483.

Gale, J. E., and J. F. Ashmore. 1994a. Charge displacement induced by rapid stretch in the basolateral membrane of the guinea pig OHC. *Proc. R. Soc. Lond. B. Biol. Sci.* 255:243–249.

Gale, J. E., and J. F. Ashmore. 1994b. An intracellular site for the inhibition of outer hair cell motility by gadolinium? Abstracts from the First International Symposium on Inner Ear Neuropharmacology, Montpellier, France, September 14–15.

Hamill, O. P., A. Marty, E. Neher, B. Sakmann, and F. R. Sigworth. 1981. Improved patch clamp techniques for high resolution current recording from cells and cell-free membrane patches. *Pflugers Arch.* 391:85–105.

Harada, N. A. Ernst, and H. P. Zenner. 1993. Hyposmotic activation hyperpolarizes outer hair cells of the guinea pig cochlea. *Brain Res.* 614:205–211.

Holley, M. C., and J. F. Ashmore. 1990. Spectrin, actin and the structure of the cortical lattice in mammalian cochlear outer hair cells. *J. Cell Sci.* 96:283–291.

Huang, G.-J., and J. Santos-Sacchi. 1993. Mapping the distribution of the outer hair cell motility voltage sensor by electrical amputation. *Biophys. J.* 65:2228–2236.

Huang, G.-J., and J. Santos-Sacchi. 1994. Motility voltage sensor of the outer hair cell resides within the lateral plasma membrane. *Proc. Natl. Acad. Sci. USA.* 91:12268–12272.

Hudspeth, A. J., and P. G. Gillespie. 1994. Pulling springs to tune transduction: adaptation by hair cells. *Neuron.* 12:1–9.

Iwasa, K. H. 1993. Effect of stress on the membrane capacitance of the auditory outer hair cell. *Biophys. J.* 65:492–498.

Iwasa, K. H. 1994. A membrane motor model for the fast motility of the OHC. *J. Acoust. Soc. Am.* 96:2216–2224.

Iwasa, K. H., and R. S. Chadwick. 1992. Elasticity and active force generation of cochlear outer hair cells. *J. Acoust. Soc. Am.* 6:3169–3173.

Iwasa, K. H., M. Li, M. Jia, and B. Kachar. 1991. Stretch sensitivity of the lateral wall of the auditory outer hair cell. *Neurosci. Lett.* 133:171–174.

Kakehata, S., T. Nakagawa, T. Takasaka, and N. Akaike. 1993. Cellular mechanism of Ach-induced response in dissociated OHCs of guinea pig cochlea. *J. Physiol.* 463:227–244.

Kalinec, F., M. C. Holley, K. H. Iwasa, D. J. Lim, and B. Kachar. 1992. A membrane based force generation mechanism in auditory sensory cells. *Proc. Natl. Acad. Sci. USA.* 89:8671–8675

Keynes, R. D., and E. Rojas. 1974. Kinetics and steady state properties of the charged system controlling sodium conductance in the squid giant axon. *J. Physiol.* 239:393–434.

Kolthoff, I. M., E. B. Sandell, E. J. Meeham, and S. Bruckenstein. 1969. Quantitative Chemical Analysis, 4th ed. The Macmillan Co., London.

Murase, K., M. Randic, T. Shirasaki, T. Nakagawa, and N. Akaike. 1990. Serotonin suppresses N-methyl-D-aspartate responses in acutely isolated rat spinal dorsal horn neurons. *Brain Res.* 525:84–91.

Ratnanather, J. T., W. E. Brownell, and A. S. Popel. 1993. Mechanical properties of the outer hair cell. *In* Biophysics of Hair Cell Sensory Systems. H. Duifhuis, J. W. Horst, P. van Dijik, and S. M. van Netten, editors. World Scientific, Singapore, 199–206.

Ruggero, M. A. 1992. Responses to sound of the basilar membrane of the mammalian cochlea. *Neurobiology.* 2:449–456.

Santos-Sacchi, J. 1989. Asymmetry in voltage dependent movements of isolated outer hair cells from the organ of Corti. *J. Neurosci.* 9:2954–2962.

Santos-Sacchi, J. 1990. Fast outer hair cell motility: how fast is fast? *In* The Mechanics and Biophysics of Hearing. P. Dallos, C. D. Geisler, J. W. Matthews, M. A. Ruggero, and C. R. Steele, editors. Springer-Verlag, Berlin, 69–75.

Santos-Sacchi, J. 1991. Reversible inhibition of voltage dependent outer hair cell motility and capacitance. *J. Neurosci.* 11:3096–3110.

Santos-Sacchi, J. 1992. On the frequency limit and phase of outer hair cell motility: effects of the membrane filter. *J. Neurosci.* 12:1906–1916.

Santos-Sacchi, J. 1993. Harmonics of outer hair cell motility. *Biophys. J.* 65:2217–2227.

Santos-Sacchi, J., and J. P. Dilger. 1988. Whole cell currents and mechanical responses of isolated outer hair cells. *Hearing Res.* 35:143–150.

Santos-Sacchi, J., G.-J. Huang, and S. Kakehata. 1994. Variability of voltage dependency of the outer hair cell (OHC) motility voltage sensor. *J. Acoust. Soc. Am.* 95:2841.

Santos-Sacchi, J., and S. Kakehata. 1994. Membrane tension directly shifts the voltage dependence of OHC gating charge and motility. Hot Poster Session, 1994 Meeting of the American Society for Cell Biology, San Francisco, December.

Shehata, W., W. E. Brownell, and R. Dieler. 1991. Effects of salicylate on shape, electromotility and membrane characteristics of isolated hair cells from the guinea pig cochlea. *Acta Oto-Laryngol. (Stockholm).* 111:707–718.

Sokabe, M., F. Sachs, and Z. Jing. 1991. Quantitative video microscopy of patch clamped membranes stress, strain, capacitance, and stretch channel activation. *Biophys. J.* 59:722–728.

Yang, X. C., and F. Sachs. 1989. Block of stretch activated ion-channels in *Xenopus* oocytes by gadolinium and calcium ions. *Science.* 243:1068–1070.